

High energy neutrino signals of four neutrino mixing

Sharada Iyer Dutta¹, Mary Hall Reno² and Ina Sarcevic¹

¹*Department of Physics, University of Arizona, Tucson, Arizona 85721*

²*Department of Physics and Astronomy, University of Iowa, Iowa City, Iowa 52242*

We evaluate the upward shower and muon event rates for two characteristic four neutrino mixing models for extragalactic neutrinos, as well as for the atmospheric neutrinos, with energy thresholds of 1 TeV, 10 TeV and 100 TeV. We show that by comparing the shower to muon event rates, one can distinguish between oscillation and no-oscillation models. By measuring shower and muon event rates for energy thresholds of 10 TeV and 100 TeV, and by considering their ratio, it is possible to use extragalactic neutrino sources to determine the type of four-flavor mixing pattern. We find that one to ten years of data taking with kilometer-size detector has a very good chance of providing valuable information about the physics beyond the Standard Model.

I. INTRODUCTION

The combined results of solar, atmospheric and laboratory experiments with neutrinos, taken at face value, require a fourth neutrino species. This follows from the observation that the results of the three categories of experiments require at least three mass-squared differences δm^2 . The mass-squared difference for solar neutrino experiments is limited to $\delta m_{solar}^2 \lesssim 10^{-3} \text{ eV}^2$ [1]. The SuperKamiokande results [2] for atmospheric neutrinos require $\delta m_{atm}^2 \sim 3 \times 10^{-3} \text{ eV}^2$, and the laboratory LSND experiment [3] limits $\delta m_{LSND}^2 > 0.2 \text{ eV}^2$. While precision measurements of the invisible decay width of the Z^0 boson constrain the addition of a fourth generation neutrino species with weak interactions, they do not constrain the possibility of a sterile neutrino species mixing with the ordinary electron, muon and tau neutrinos. Analyses of solar and atmospheric experiments assuming pure $\nu_i \rightarrow \nu_s$ oscillations indicate that the data do not support the hypothesis, however, combined fits to all of the experimental data do require a sterile neutrino species [4].

Recent SuperK data on atmospheric neutrinos indicate $\nu_\mu \rightarrow \nu_\tau$ oscillations with mixing being nearly bi-maximal [2]. We have shown in Ref. [5] that for extragalactic sources of muon neutrinos, mixing with tau neutrinos in transit to the Earth leads to distinct signatures of oscillation which do not require explicit identification of a tau lepton in large underground experiments. In this paper, we investigate the signatures of neutrino oscillations in large underground experiments for models with three active neutrinos and one sterile neutrino whose mixing is constrained by lower energy experiments.

II. MIXING MODELS AND EXTRAGALACTIC FLUXES

Global fits to oscillation data fall into two distinct patterns of neutrino mixing. The first is a mass spectrum in which $\nu_e \leftrightarrow \nu_s$ with a mass splitting δm_{solar}^2 , $\nu_\mu \leftrightarrow \nu_\tau$

with δm_{atm}^2 and a splitting between the two nearly degenerate pairs characterized by δm_{LSND}^2 . The approximate mixing matrix in this scenario has the form [4]

$$\begin{pmatrix} \nu_s \\ \nu_e \\ \nu_\mu \\ \nu_\tau \end{pmatrix} = \begin{pmatrix} \frac{1}{\sqrt{2}} & \frac{1}{\sqrt{2}} & 0 & 0 \\ -\frac{1}{\sqrt{2}} & \frac{1}{\sqrt{2}} & \epsilon & \epsilon \\ \epsilon & -\epsilon & \frac{1}{\sqrt{2}} & \frac{1}{\sqrt{2}} \\ 0 & 0 & -\frac{1}{\sqrt{2}} & \frac{1}{\sqrt{2}} \end{pmatrix} \begin{pmatrix} \nu_0 \\ \nu_2 \\ \nu_2 \\ \nu_3 \end{pmatrix}, \quad (1)$$

where $\epsilon < 0.1$ [4]. Following Ref. [4], we call this a 2 + 2 scenario.

The second pattern of neutrino mass and mixing, allowed by the most recent analysis of the LSND experiment, has large mixing between the three ordinary neutrinos and a small mixing with the sterile neutrino, characterized by small parameters ϵ and δ . A characteristic mixing matrix has the form [4]

$$\begin{pmatrix} \nu_s \\ \nu_e \\ \nu_\mu \\ \nu_\tau \end{pmatrix} = \begin{pmatrix} 1 & \frac{\delta}{2} - \frac{\epsilon}{\sqrt{2}} & -\frac{\delta}{2} - \frac{\epsilon}{\sqrt{2}} & -\frac{\delta}{\sqrt{2}} \\ \epsilon & \frac{1}{\sqrt{2}} & \frac{1}{\sqrt{2}} & 0 \\ \delta & -\frac{1}{2} & \frac{1}{2} & \frac{1}{\sqrt{2}} \\ 0 & \frac{1}{2} & -\frac{1}{2} & \frac{1}{\sqrt{2}} \end{pmatrix} \begin{pmatrix} \nu_0 \\ \nu_2 \\ \nu_2 \\ \nu_3 \end{pmatrix}. \quad (2)$$

Following Ref. [4], we call this a 1 + 3 scenario.

For extragalactic sources, because of the large distances involved, the oscillation flavor ratios are essentially independent of mass-squared differences and neutrino energy, since

$$\langle \sin^2 \left(\frac{1.27 \delta m^2 L}{E} \right) \rangle \simeq \frac{1}{2}, \quad (3)$$

for δm^2 in eV^2 , L in km, and E in GeV. Consequently, the oscillation probabilities can be written as

$$P(\nu'_\ell \rightarrow \nu_\ell) = \sum_j |U_{\ell j}|^2 |U_{\ell' j}|^2, \quad (4)$$

in terms of the elements of the neutrino mixing matrix $U_{\ell j}$. The ν_ℓ flux in detectors F_ℓ^D , in terms of the fluxes at the source F_ℓ^S are [6]

$$F_{\nu_\ell}^D = \sum_{\ell'} P(\nu_{\ell'} \rightarrow \nu_\ell) F_{\nu_{\ell'}}^S. \quad (5)$$

As we discuss below, our “source” fluxes are actually summed over many sources to yield isotropic fluxes. We continue to denote these isotropic fluxes, unmodified by oscillations, as the source fluxes.

Given source ratios of fluxes $\nu_s^S : \nu_e^S : \nu_\mu^S : \nu_\tau^S = 0 : 1 : 2 : 0$ yield different ratios of neutrino fluxes at the detector, depending on whether the 2+2 or 1+3 scenario describes four-neutrino mixing. In the 1+3 case with small ϵ and δ , the detector ratios are approximately $0 : 1 : 1 : 1$, while for the 2+2 case, sterile neutrinos make an important component of the flux at the Earth, with $\nu_s^D : \nu_e^D : \nu_\mu^D : \nu_\tau^D \simeq 0.5 : 0.5 : 1 : 1$. With three neutrino species and bi-maximal mixing, one finds $\nu_e^D : \nu_\mu^D : \nu_\tau^D \simeq 1 : 1 : 1$. Without mixing, the source fluxes and detector fluxes have the same flavor ratios of $1 : 2 : 0$. As a result, the 1+3 scenarios essentially reproduce the three-flavor bi-maximal mixing scenario, while the 2+2 scenarios lie between the 3-flavor bi-maximal mixing model and the no-mixing model.

There are a variety of predictions for isotropic neutrino fluxes from active galactic nuclei (AGN), gamma ray bursters (GRB) and models with topological defects. A sample of these predictions for muon neutrino plus antineutrino fluxes, in the absence of oscillations, are shown in Fig. 1. These include the AGN models of Stecker and Salamon (AGN_SS) [7] and of Mannheim Model A (AGN_M95) [8]. GRB predictions are represented by the Waxman-Bahcall model of Ref. [9] (GRB_WB). Two topological defect models, from Sigl, Lee, Schramm and Coppi (TD_SLSC) [10] and Wichoski, MacGibbon and Brandenberger (TD_WMB) [11] are also shown. We include fluxes with energy behaviors like $1/E$ and $1/E^2$ as well. We chose normalization for each of these fluxes consistent with the current limits [14], $F_{\nu_\mu}^S = 10^{-12} (E/\text{GeV})^{-1} \text{GeV}^{-1} \text{cm}^{-2} \text{sr}^{-1} \text{s}^{-1}$ and $F_{\nu_\mu}^S = 10^{-6} (E/\text{GeV})^{-2} \text{GeV}^{-1} \text{cm}^{-2} \text{sr}^{-1} \text{s}^{-1}$ (in which the fluxes include neutrinos and antineutrinos in equal amounts and correspond to the initial fluxes before accounting for oscillations). The E^{-1} flux is smoothly cut off at high energies, as indicated in Fig. 1.

For comparison, the hatched curve shows the angle-dependent atmospheric flux (ATM) [12]. Because of the dominance of the atmospheric flux below 1 TeV energies, we restrict our consideration to $E > 1 \text{ TeV}$.

In Ref. [5], for muon neutrinos, we have taken these representative fluxes and evaluated how neutrino interactions in the Earth modify the neutrino fluxes with the regeneration attributed to the neutral current interactions. In addition, for tau neutrinos, we describe the extent to which neutral current interactions and charged current production of τ followed by its decay, regenerate neutrinos. There, we make a detailed numerical evaluation of the “pile-up” of tau neutrinos that was discussed by Halzen and Saltzberg in Ref. [13]. In the next section, we use the neutrino fluxes of Fig. 1 modified due to their

passage through the Earth [5] in the appropriate flavor proportions for the 1+3 and 2+2 scenarios.

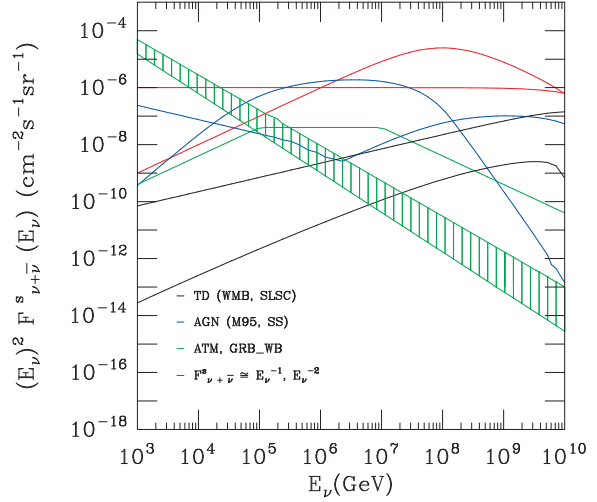


FIG. 1. Isotropic muon neutrino plus antineutrino flux predictions for a variety of extragalactic models (see text), scaled by neutrino energy squared. The antineutrino flux is taken equal to the neutrino flux.

III. UNDERGROUND SIGNATURES

Backgrounds from atmospheric muons make downward event rates difficult to extract, so our focus is on upward events. Two types of events will be produced: muon events and shower events. The muon events come from upward muons from $\nu_\mu \rightarrow \mu$ charged current events and from $\nu_\tau \rightarrow \tau \rightarrow \mu X$ from charged current production of taus followed by a muonic decay. In spite of the pile-up in the tau neutrino flux, the net effect of oscillations is to reduce the muonic event rate by approximately a factor of two relative to the no-oscillation rate, whether in the 1+3 or 2+2 mixing scenario. Details for how the rates are calculated appear in Ref. [5]. Given the uncertainties in the normalizations of the extragalactic fluxes (unlike the atmospheric flux), the muon event rate is not enough to distinguish oscillation scenarios from no-oscillation scenarios.

The distinction between oscillation and no-oscillation scenarios comes by comparing the muon rate with the shower rate. The principle of this procedure is very similar to what some experiments will be able to do with low energy neutrinos: namely, to compare the neutral current rate to the charge current interaction rate. In large neutrino telescopes, tau identification is difficult, and we assume that showers of hadronic and electromagnetic origin cannot be distinguished. Consequently, the shower rate comes from the following processes from neutrino-nucleon (N) interactions:

$$\begin{aligned}
&\nu_\tau N \rightarrow \tau + \text{hadrons}, \tau \rightarrow \nu_\tau + \text{hadrons}, \\
&\nu_\tau N \rightarrow \tau + \text{hadrons}, \tau \rightarrow \nu_\tau + e + \nu_e, \\
&\nu_\tau N \rightarrow \nu_\tau + \text{hadrons}, \\
&\nu_{e,\mu} N \rightarrow \nu_{e,\mu} + \text{hadrons}, \\
&\nu_e N \rightarrow e + \text{hadrons}.
\end{aligned} \tag{6}$$

The shower energy is taken as the sum of hadronic and electron energies including both the production vertex and the decay vertex, where applicable.

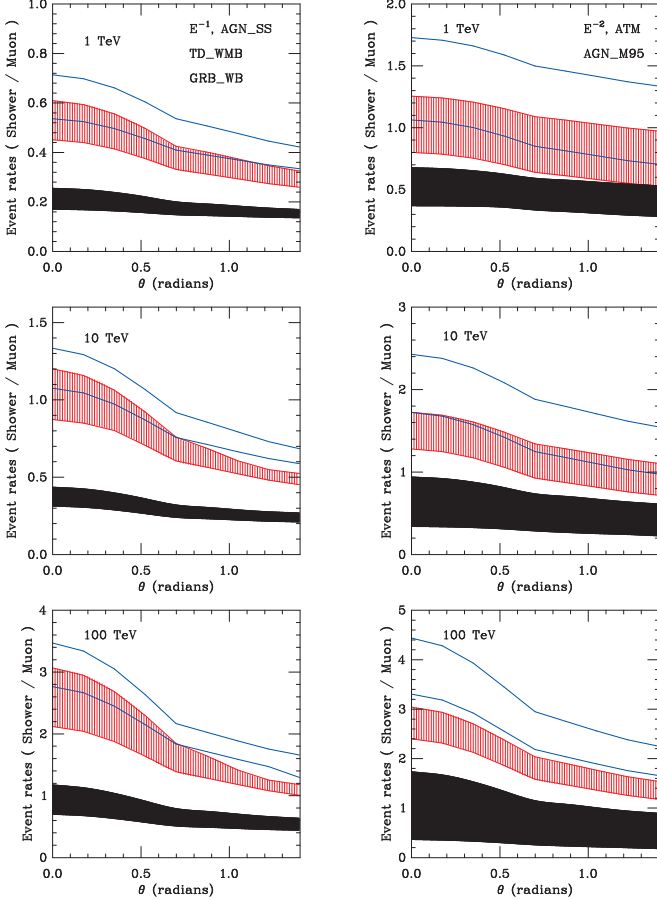


FIG. 2. Ratio of shower event rates to muon event rates for the 1 + 3, 2 + 2 and no oscillation scenarios as a function of nadir angles for threshold energies of 1 TeV, 10 TeV and 100 TeV, for the indicated fluxes. The blue lines bracket the 1 + 3 scenario, the red shaded area represents the 2 + 2 scenario and the black shaded area represents no-mixing case for the given fluxes.

The ratio of the shower rate to the muon rate for the extragalactic flux models of Fig. 1 are used to bracket the theoretical expectations for the ratio in 2 + 2 and 1 + 3 mixing models, and compared with the standard model expectations. As in Ref. [5], we separate the flux models into two categories: more steeply falling fluxes (E^{-2} , ATM and the Mannheim AGN flux) and the less steep behavior of the other five sample fluxes of Fig. 1. Experimentally, the steeply falling fluxes are character-

ized by the muon event rate nadir angle dependence and the threshold energy dependence, which differ from the models with a weaker energy dependence. The two separate categories of fluxes, for threshold energies of 1, 10 and 100 TeV are shown in Figs. 2 (a-f). The 1 + 3 models are bracketed by the black lines, the 2 + 2 models with the red and the standard model with the blue.

For the 1 TeV threshold, the 1 + 3 and 2 + 2 event rates as a function of nadir angle overlap for both energy behaviors of the input fluxes. The no-oscillation band lies below the oscillation bands with the exception of the near horizontal rates in the steeply falling flux category (labeled E^{-2}). The separation between the oscillation and no-oscillation scenarios is better for higher thresholds, looking only in terms of the theoretical ratio of shower to muon event rates. However, the higher thresholds have lower event rates overall.

IV. DISCUSSION

In Tables I-III we present our results for the shower and muon event rates integrated over the nadir angle for energy thresholds of 1 TeV, 10 TeV and 100 TeV and for a kilometer-size detector. We do not include the topological defect models in these figures because the event rates are so low. For the 1 TeV threshold, only 0.1 – 0.2 upward muon events are predicted per year for a km² instrumented area for the TD_WMB model. In all cases, we have considered shower rates in a km³ volume, and muon rates/km² (where the average muon range [15] provides the additional space dimension). Clearly the two oscillation scenarios give muon event rates but very different shower rates. With an energy threshold of 1 TeV, we find that AGN fluxes could, in principle, provide a clear distinction between different oscillation scenarios, as well as to separate the no oscillation case. From Table I, we note that for 1 TeV energy threshold, atmospheric background is large. However, as seen in Fig. 3, over the period of five years, the statistical errors on extragalactic fluxes can be sufficiently reduced so that the ratio of showers to muons, in combination with overall upward muon rates, could be used to discriminate two oscillation scenarios. In Figs. 3-5, we show ratio of the shower to muon event rates integrated over nadir angles for energy thresholds of 1 TeV, 10 TeV and 100 TeV for a variety of fluxes and for different oscillation scenarios. The error bars are estimated with the assumption of a Poisson distribution, leading to

$$\sigma_R = R \sqrt{\frac{1}{N_{shr}} + \frac{1}{N_\mu}} \tag{7}$$

where R is the ratio of shower to muon events.

From Fig. 3 and Table I, we note that AGN fluxes, as well as E^{-2} and E^{-1} fluxes, would have the best possibility of separating different oscillation scenarios by detecting the showers and muons in kilometer-size detector over

the period of one to two years, assuming a good understanding of the atmospheric muon neutrino and electron neutrino fluxes. The GRB_WB flux would require five years of data to reduce statistical errors so that the error bars do not overlap for the two oscillation scenarios.

The shower and muon event rates for an energy threshold of 10 TeV are shown in Table II. The AGN model of Stecker and Salamon predicts large shower and muon rates, and order of magnitude larger than the atmospheric background. The AGN model of Mannheim and the GRB model of Waxman and Bahcall predict rates to be about half of the background, while E^{-2} and E^{-1} fluxes give significantly more events than the atmospheric background when oscillations are taken into account. Thus, there is a possibility of detecting extragalactic neutrinos by imposing a 10 TeV energy threshold [5]. In addition, one can consider the ratio of shower and muon events with the 10 TeV energy threshold for determining oscillation scenario, as indicated in Fig. 4. We note that for the GRB_WB and AGN_M95 fluxes, it would be necessary to take data for six and four years respectively to separate error bars for the two oscillation scenarios.

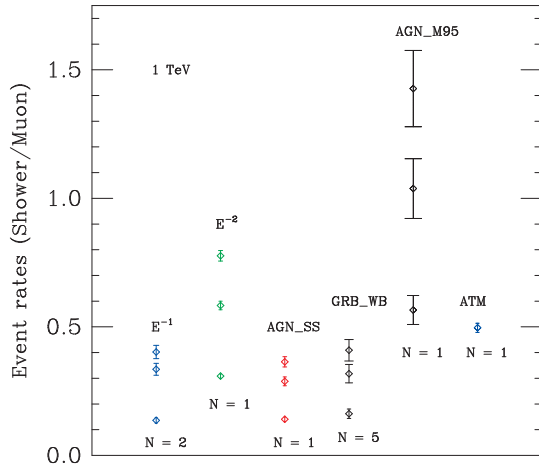


FIG. 3. Integrated over solid angle, the ratio of upward shower to muon event rates for given flux models for a threshold energy of 1 TeV. The error bars are determined assuming N years of data taking.

If the energy threshold is increased to 100 TeV, the atmospheric background is negligible. This can be seen from Table III. The shower and muon event rates are several hundreds for AGN_SS model, while for all other models the rates are much smaller, but still significant for kilometer-size detector in a time period of one year. Furthermore, the ratio of the shower and muon events can clearly separate oscillation and no oscillation scenarios, as well as distinguish two oscillations scenarios that

we consider. In Fig. 5 we show this ratio including statistical errors. We find that even with error bars it still seems possible to distinguish between different oscillation scenarios. However, in order to reduce statistical errors,

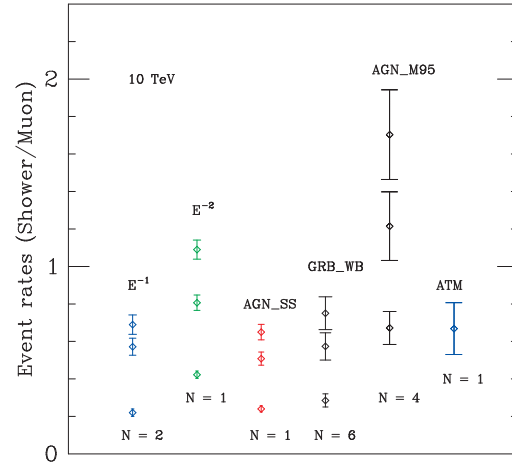


FIG. 4. Integrated over solid angle, the ratio of upward shower to muon event rates for given flux models for a threshold energy of 10 TeV. The error bars are determined assuming N years of data taking.

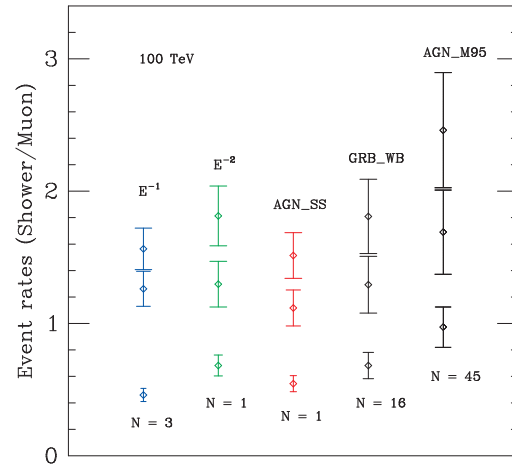


FIG. 5. Integrated over solid angle, the ratio of upward shower to muon event rates for given flux models for a threshold energy of 100 TeV. The error bars are determined assuming N years of data taking.

the GRB_WB flux prediction would require collecting data for more than a decade. On the other hand, one year is sufficient for the AGN_SS flux. In case of an E^{-1}

flux, we expect several hundreds of showers and muons over the period of three years, which is necessary in order to reduce error bars to the point of being able to distinguish oscillation scenarios. For a steeper flux, E^{-2} , one year is sufficient to get enough events as well as to reduce the statistical errors at the current AMANDA limit on the isotropic flux normalization.

V. CONCLUSION

We have shown that measurements of the upward showers and muons, and considering their ratio, with the kilometer-size detector, could provide very good test of different oscillation scenarios. Taking into account statistical errors, we find that generic fluxes, such as $F_{\nu_\mu}^S = 10^{-12} (E/\text{GeV})^{-1} \text{GeV}^{-1} \text{cm}^{-2} \text{sr}^{-1} \text{s}^{-1}$ and $F_{\nu_\mu}^S = 10^{-6} (E/\text{GeV})^{-2} \text{GeV}^{-1} \text{cm}^{-2} \text{sr}^{-1} \text{s}^{-1}$, with energy threshold of 10 TeV and 100 TeV, would have enough statistics in one to two years of data taking to distinguish not only between oscillation and no oscillation scenario, but also whether it is $2+2$ or $1+3$ model. The AGN model of Stecker-Salamon [7], with a 10 TeV energy threshold predicts between 600 and 1000 muons/km² per year and between 260 and 400 shower events/km³ per year, with clear separation between different oscillation scenarios. The other AGN model, proposed by Mannheim [8], predicts less events and would require four years to reduce statistical errors in the ratio of shower to muon event rates such that there is clear distinction between not only the no oscillation and oscillation cases, but also different oscillation models. If we want to use GRB.WB flux [9] to test these models, it would take five to six years with the kilometer-size detector to get sufficient statistics. A higher energy threshold of 100 TeV makes the atmospheric neutrino background negligible, but event rates for extragalactic neutrinos are also reduced. Still, the AGN.SS model would be able to provide valuable information about the oscillation scenario, as well as E^{-2} flux in just one year of data, while an E^{-1} flux with our normalization would need three years. Other fluxes, such as GRB.WB and AGN.M95 flux would require much longer time.

The assumption of the existence of sterile neutrino is necessary to explain the solar, atmospheric, reactor and accelerator data. The MiniBooNE experiment [16] will search for $\nu_\mu \rightarrow \nu_e$ oscillations and test the LSND results. The presence of the sterile neutrino in the $2+2$ model will be tested by the measurement of the suppression of NC/CC ratio of the solar neutrinos by the SNO experiment [17], whereas $1+3$ model can be tested by searches from small amplitude oscillations at short baseline experiment such as ORLAND [18].

Observation of the flavor ratio of extragalactic neutrinos could serve as a complementary test for oscillation models that incorporate sterile neutrinos. Oscillations of neutrinos from astronomical sources are averaged over

very long baseline and thus cannot provide any direct information about the neutrino mass. However, we have shown that extragalactic neutrinos could be used to distinguish between different oscillation scenarios. The observed muon and shower event distributions as a function of angle and energy threshold will help determine the energy behavior of the incident extragalactic neutrino flux and point to a model or class of models for their sources. Combined measurements of the upward showers and muons and, in particular, their ratio provides a basic test of the oscillation scenario.

Acknowledgments

The work of S.I.D. and I.S. has been supported in part by the DOE under Contracts DE-FG02-95ER40906 and DE-FG03-93ER40792. The work of M.H.R. has been supported in part by National Science Foundation Grant No. PHY-9802403.

-
- [1] Y. Suzuki, Nucl. Phys. Proc. Suppl. **91**, 29 (2001); B. T. Cleveland *et al.*, Nucl. Phys. Proc. Suppl. **38**, 47 (1995); J. N. Abdurashitov *et al.* [SAGE Collaboration], Phys. Rev. C **60**, 055801 (1999) [astro-ph/9907113]; T. A. Kirsten [GALLEX and GNO Collaborations], Nucl. Phys. Proc. Suppl. **77**, 26 (1999).
 - [2] Y. Fukuda *et al.* [Super-Kamiokande Collaboration], Phys. Rev. Lett. **81**, 1562 (1998) [hep-ex/9807003].
 - [3] C. Athanassopoulos *et al.* [LSND Collaboration], Phys. Rev. Lett. **81**, 1774 (1998) [nucl-ex/9709006]; C. Athanassopoulos *et al.* [LSND Collaboration], Phys. Rev. Lett. **77**, 3082 (1996) [nucl-ex/9605003]. I. Stancu [LSND Collaboration], Nucl. Phys. Proc. Suppl. **85**, 78 (2000).
 - [4] V. Barger, B. Kayser, J. Learned, T. Weiler and K. Whisnant, Phys. Lett. B **489**, 345 (2000) [hep-ph/0008019].
 - [5] S. Iyer Dutta, M. H. Reno and I. Sarcevic, Phys. Rev. D **62**, 123001 (2000) [hep-ph/0005310].
 - [6] D. V. Ahluwalia, C. A. Ortiz and G. Z. Adunas, hep-ph/0006092.
 - [7] F. W. Stecker and M. H. Salamon, Space Sci. Rev. **75**, 341 (1996) [astro-ph/9501064].
 - [8] K. Mannheim, Astropart. Phys. **3**, 295 (1995).
 - [9] E. Waxman and J. Bahcall, Phys. Rev. D **59**, 023002 (1999) [hep-ph/9807282].
 - [10] G. Sigl, S. Lee, D. N. Schramm and P. Coppi, Phys. Lett. B **392**, 129 (1997) [astro-ph/9610221].
 - [11] U. F. Wichoski, J. H. MacGibbon and R. H. Brandenberger, hep-ph/9805419.
 - [12] V. Agrawal, T. K. Gaisser, P. Lipari and T. Stanev, Phys. Rev. D **53**, 1314 (1996) [hep-ph/9509423].
 - [13] F. Halzen and D. Saltzberg, Phys. Rev. Lett. **81**, 4305 (1998) [hep-ph/9804354]; S. Iyer, M. H. Reno and I. Sarcevic, Phys. Rev. D **61**, 053003 (2000) [hep-ph/9909393]; F. Becattini and S. Bottai, astro-

ph/0003179.

- [14] E. Andres *et al.* [AMANDA Collaboration], Nucl. Phys. Proc. Suppl. **91**, 423 (2000) [astro-ph/0009242].
- [15] P. Lipari and T. Stanev, Phys. Rev. D **44**, 3543 (1991).
- [16] A. Bazarko [MiniBooNE Collaboration] Nucl. Phys. Proc. Suppl. **91**, 210-215 (2001) [hep-ex/0009056].
- [17] A. McDonald [SNO Collaboration] Nucl. Phys. Proc. Suppl. **91**, 21-28 (2001) [hep-ex/0011025].
- [18] F. Avignone [ORLaND Collaboration] Nucl. Phys. Proc. Suppl. **91**, 113-119 (2001) [hep-ex/0011025].

TABLE I. Integrated upward shower (muon) rates per year for energy threshold of 1 TeV.

Model	E^{-1}	E^{-2}	AGN_SS	AGN_M95	GRB_WB	ATM
1+3	170(422)	2530(326)	459(1260)	224(157)	26.9(65.8)	
2+2	141(422)	1900(3260)	363(1260)	163(157)	20.9(65.8)	
No osc	88.1(646)	1750(5680)	297(2110)	158(280)	18.3(113)	1170(2360)

TABLE II. Integrated upward shower (muon) rates per year for energy threshold of 10 TeV.

Model	E^{-1}	E^{-2}	AGN_SS	AGN_M95	GRB_WB	ATM
1+3	150(217)	954(875)	405(623)	34.4(20.2)	21.3(28.4)	
2+2	124(217)	706(875)	316(623)	24.5(20.2)	16.3(28.4)	
No osc	75.4(342)	652(1540)	257(1070)	24.4(36.3)	14.2(49.7)	39.1(58.5)

TABLE III. Integrated upward shower (muon) rates per year for energy threshold of 100 TeV.

Model	E^{-1}	E^{-2}	AGN_SS	AGN_M95	GRB_WB	ATM
1+3	84.8(54.2)	182(100)	193(128)	2.46(0.999)	7.28(4.03)	
2+2	68.4(54.2)	130(100)	143(128)	1.69(0.999)	5.21(4.03)	
No osc	42.0(91.3)	124(182)	125(230)	1.78(1.83)	4.99(7.31)	0.66(0.77)